Applied Physics A (2023) 129:714
https://doi.org/10.1007/s00339-023-06977-4

Applied Physics A
Materials Science & Processing

Laser generation of $CeAlO_3$ nanocrystals with perovskite structure

Volodymyr Vasylkovskyi[1,2,3] · Iryna Bespalova[1,3] · Oleksandr Gryshkov[3,4] · Mykola Slipchenko[1,3] · Serhii Tkachenko[1] · Pavlo Arhipov[1] · Iaroslav Gerasymov[1] · Yuriy Zholudov[5] · Zhijun Zhao[6] · Armin Feldhoff[6] · Aleksander Sorokin[1] · Olena Slipchenko[2,3] · Borys Grynyov[1] · Boris Chichkov[3]

Received: 1 June 2023 / Accepted: 1 September 2023 / Published online: 20 September 2023

Abstract
For the first time to the best of our knowledge, $CeAlO_3$ nanocrystals with perovskite structure are synthesized by pulsed laser ablation technique. The morphological and optical properties of the obtained $CeAlO_3$ nanocrystals are investigated. This work opens new prospects for the application of laser ablation methods for the generation of perovskite nanocrystals and development of novel nanocomposite structures, which can be applied for the fabrication of perovskite solar cells, scintillation detectors, catalysts, etc.

Keywords $CeAlO_3$ · Perovskite · Laser ablation · Scintillation nanocrystals

1 Introduction

Pulsed laser ablation (PLA) is a physical approach that has attracted considerable attention by enabling the generation of nanoparticles (NPs) with various structures and compositions as well as highly pure NPs surfaces. PLA technique is based on the application of laser pulses focused on the surface of a target material for the generation of NPs (Fig. 1). Laser techniques can offer good universality, scalability and high reproducibility of synthesis process. PLA generation of chemically clean and eco-friendly nanoparticles has evolved into the research field attracting laboratory and industrial applications [1].

PLA can be conducted in vacuum, gaseous, and liquid media [2]**.** Parameters of liquids (type, viscosity, temperature, compressibility, etc.) influence the properties of the cavitation bubble (expansion, volume, velocity, lifetime) that traps nanoparticles generated during the ablation process. The cavitation properties also affect melting and growth of NPs [3]. PLA in liquids is more promising because of its versatility, safety and ease of execution [4, 5]. This technique offers the size and shape control of the obtained NPs by tuning laser and surfactant parameters. Using this method opens up possibilities for the generation and investigation of novel nanomaterials, including those that cannot be or have not been synthesized by chemical techniques.

PLA method has already been used for the generation of NPs from metals, semiconductors, ceramics, alloys**,** and multicomponent crystalline structures including scintillation materials [5–8]. A scintillator is a type of material that converts various kinds of high-energy radiation (X-rays, gamma-rays, alpha-rays, beta-rays, electron rays, proton rays, heavy particle rays, neutron rays, etc. [9–11]) into visible light. Such materials are usually applied as single crystals and used as detectors in high-energy physics, medical diagnostics, security applications, etc. At present, investigations towards new fast scintillation materials with better

✉ Volodymyr Vasylkovskyi
volodymyr.vasylkovskyi@khpi.edu.ua

1 Institute for Scintillation Materials of the National Academy of Sciences of Ukraine, Nauky Ave. 60, Kharkiv 61072, Ukraine

2 Department of Metals and Semiconductors Physics, National Technical University "Kharkiv Polytechnic Institute", Kyrpychova Str. 2, Kharkiv 61002, Ukraine

3 Institute of Quantum Optics, Leibniz University Hannover, Welfengarten 1, 30167 Hannover, Germany

4 Lower Saxony Center for Biomedical Engineering, Implant Research and Development, Stadtfelddamm 34, 30625 Hannover, Germany

5 Department of Biomedical Engineering, Kharkiv National University of RadioElectronics, Nauky Ave. 14, Kharkiv 61166, Ukraine

6 Institute of Physical Chemistry and Electrochemistry, Leibniz University Hannover, Callinstrasse 3A, 30167 Hannover, Germany

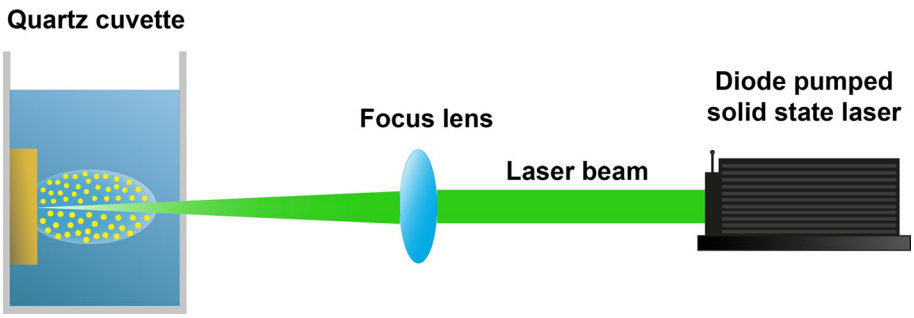

Fig. 1 Scheme of PLA synthesis of nanocrystals

characteristics for the development of novel scintillation detectors are in progress. Recent research on PLA generation of multicomponent crystalline nanostructures included oxide and garnet scintillators doped with Eu and Ce [5, 7] and in a smaller degree halide perovskites [12]. The obtained garnet NPs partially or fully retained their crystalline structure and optical properties, compared to the bulk materials. Also, at constant laser parameters, it has been observed that the higher the melting temperature of the target crystal, the larger is the average size of the obtained scintillation nanoparticles [5]. R. A. Rajan et al. reported on the research of femtosecond laser processing of $MAPbX_3$ ($MA = CH_3NH_3$, X = Br, I, and Cl), where PLA of single crystal resulted in the generation of recrystallized micro- and nanostructures which exhibited amplified spontaneous emission [12].

$CeAlO_3$ crystals attract much attention for their ferroelectric, optical, and luminescent properties and quite a fast scintillation response under α-particle excitation (decay time ≈ 56 ns). $CeAlO_3$ NCs have been previously synthesized by solution-combustion route [12], sol–gel technique [14] and high-temperature (873 K) reaction of CeO_2 nanoparticles supported on Al_2O_3 [15]. $CeAlO_3$ NCs could be potentially applied in catalysts for biogas reforming [15, 16], wound dressing materials [17], optical and scintillation detector systems [9], etc. In combination with radiation-resistant polymers, $CeAlO_3$ NCs could be used for the fabrication of fast scintillation detectors. $CeAlO_3$-containing nanocomposites can be applied in catalysts for biogas reforming, where $CeAlO_3$ increases the rate of carbon gasification. Shahverdi et. al. reported that $CeAlO_3$ NCs incorporation in biaxial electrospun nanofibers based on chitosan-poly (vinyl alcohol) and poly (Ɛ-caprolactone) can improve mechanical, drug delivery, and biological response properties of the potential wound dressing materials [17].

In this paper, we apply the PLA technique on the cerium aluminate oxide ($CeAlO_3$) single crystal with a perovskite crystal structure for the generation of $CeAlO_3$ nanocrystals (NCs). In this work, we demonstrate the possibility of obtaining ultrapure $CeAlO_3$ NCs by the PLA technique. The retaining of crystal structure and improvement of optical properties compared to the bulk material are demonstrated. Possible applications of the obtained NCs are discussed.

2 Materials and methods

2.1 $CeAlO_3$ single crystal

The growth of a $CeAlO_3$ oxide perovskite single crystal (Fig. 2) was conducted by the edge defined film-fed growth (EFG) technique in an induction heating furnace "OXIDE". The crystal was obtained from a tungsten crucible using a round Mo shaper in Ar + CO reducing atmosphere. The fabrication process is described in more detail in [P. Arhipov et al. 2015] [9, 10].

2.2 PLA setup

For the PLA synthesis of $CeAlO_3$ NCs, a nanosecond diode-pumped laser Alphalas PULSELAS P-355–100-HP with the following parameters: $\lambda \approx 1064$ nm; $\Delta t \approx 845$ ns; repetition rate ≈ 560 Hz, beam spot size ≈ 0.203 mm, pulse energy ≈ 212 μJ (laser fluence ≈ 1.31 J/cm^2), with vertical polarization of the laser beam was used. During the PLA process, laser beam was focused by an optical lens with a focal distance of 60 mm on the surface of the $CeAlO_3$ single crystal that was placed in a quartz cuvette. A simplified scheme of the PLA synthesis of $CeAlO_3$ NCs is illustrated in Fig. 1.

In our experiments we used: a stable laser system operating in an environment with a constant temperature; liquids with constant parameters; single crystal, stable in the investigated liquids. Therefore, the experimental error may be only related to the power instability of the laser (< 2% rms, 1 h).

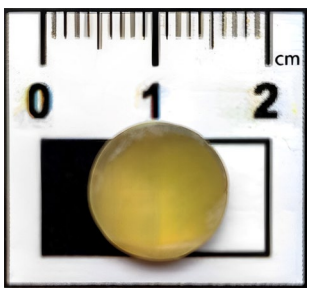

Fig. 2 Fragment of $CeAlO_3$ single crystal

2.3 Choice of liquid medium for PLA

The choice of liquid medium for PLA has an important role since it influences the ablation process, formation of byproducts, stability of NP colloid, and convenience of further NPs application [5, 18]. Preliminary experiments were conducted in order to select the most suitable medium for PLA generation of $CeAlO_3$ NCs. As a media for PLA and for $CeAlO_3$ NCs storage chloroform (99.8%, Carl Roth GmbH + Co. KG, Germany), toluene (≥ 99.8%, GC Ultra Grade Carl Roth GmbH + Co. KG, Germany), and distilled water (Laboratory ultra-pure water purification unit – Milli-Q Integral system, Merck Millipore, Germany) were used without further purification.

Parameters of the liquid environment (type, viscosity, temperature, compressibility, etc.) for PLA and its purity can strongly affect the composition, shape, and size of the obtained NCs. In this work, PLA of $CeAlO_3$ was conducted at room temperature in water and organic solvents (toluene and chloroform). However, fluid purity is an important issue and, for example, high-pressure liquid chromatography or spectroscopy solvents may contain atmospheric gases such as N_2, O_2, H_2O, and CO_2, as well as traces of other compounds. Water also contains O_2 and N_2 under atmospheric conditions. In specific cases, the degradation over time of the solvent may give by-products. Therefore, it must be taken into account that various types of impurities are present during PLA, even if solvents for spectroscopy and high-pressure liquid chromatography were used [4]. In case of the application of water as a PLA medium, colloidal solutions do not contain any by-products, which makes it a very convenient environment for the PLA process. Even though, colloidal solutions obtained by PLA in distilled water are not suitable for further applications in the form of thin films or combination with polymers compared to organic solvents. On the other hand, organic solvents after the absorption of laser irradiation can generate hydrogen, carbon, and acetyl group radicals and ions that can form unwanted products in the solution. Usually as a result of the laser breakdown of organic solvent, the amorphous carbon is produced [3]. This effect was most pronounced in toluene, where dark micro- and nanoparticles were observed in a significant amount. Taking into account the abovementioned disadvantages of distilled water and toluene, chloroform became the most convenient environment for PLA synthesis of $CeAlO_3$ NCs both because of the very low amount of by-products and the possibility of further practical applications. As a result of PLA of $CeAlO_3$ single crystal in chloroform, colloids with turbid yellow color were obtained. Such a color can be described by the presence of $CeAlO_3$ NCs and products of laser breakdown of chloroform.

2.4 Characterization of the laser generated $CeAlO_3$ NCs

For the characterization of laser generated $CeAlO_3$ NCs, the following techniques were applied: transmission electron microscopy (TEM), Fourier-transform infrared spectroscopy (FTIR), absorption and luminescence spectroscopy, luminescent decay times measurements, and the X-ray diffraction analysis (XRD). TEM images of NCs were made with TEM Tecnai G2 F20 TMP from FEI. FTIR spectroscopy was conducted using the "Spectrum Two" FTIR Spectrometer from Perkin Elmer. The John Wiley & Sons, Inc. "SpectraBase" [19] and Merck "IR Spectrum Table" [20] were used to characterize the acquired FTIR spectra. The absorption spectra were acquired with the "Hamamatsu" double beam spectrometer. The luminescent emission and excitation spectra were measured with the "HORIBA FluoroMax Plus" spectrofluorometer. Luminescence decay curves were measured using a picosecond spectrofluorimeter Fluotime 200 (PicoQuant, Germany) using a picosecond laser module with a wavelength of 379 nm, with the instrument response function of 100 ps.

The X-ray diffraction analysis has been conducted using a Bruker D8 Advance XRD diffractometer (Cu-Kα radiation having the wavelength 1.5406 Å) to reveal the crystalline structure of the laser generated nanomaterials. These measurements were conducted in Bragg–Brentano geometry in 2Theta range from 4° to 70° (0.01° per step, and 2 per step) in air at room temperature. Before measurements, the powder samples were briefly ground and spread on a sample carrier (silicon) using ethanol. The reference pattern with the ICSD collection code 72,558 of the crystalline compound was used to identify the presence of material phases.

3 Results and discussion

3.1 PLA synthesis of $CeAlO_3$ NCs

First, influence of the PLA process duration time (10 and 30 min) on the generation of NCs was investigated. It was observed that, with longer duration of the PLA process, the NCs generation initially increase, and the colloidal solution becomes more saturated, as it can be seen in Fig. 3b. However, in this case no further increase in NCs generation is observed since highly concentrated colloidal solution absorbs laser radiation shielding the single crystal target [3]. For further characterization of $CeAlO_3$ NCs, the colloidal solution obtained by 30 min long PLA was used. It corresponds to the maximum concentration of NCs of 2.5×10^{-5} g/L, which was determined by the gravimetric method.

The supernatant of the colloidal solution of $CeAlO_3$ NCs has been investigated by TEM. On TEM images,

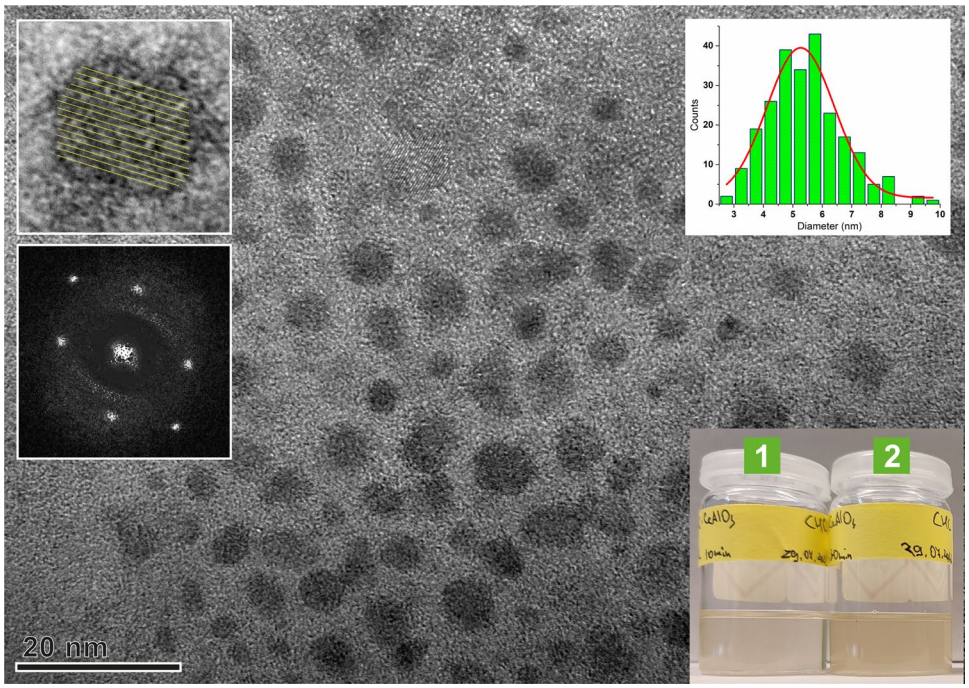

Fig. 3 TEM image of $CeAlO_3$ PeNCs obtained by PLA (PLA duration = 30 min), top-left inserts depict planes of atoms in the crystalline structure and corresponding fast Fourier transform, top-right insert shows the NCs size distribution, bottom-right insert shows an image of $CeAlO_3$ NCs colloidal solutions obtained in chloroform by PLA: (1) PLA duration – 10 min, (2) PLA duration – 30 min

partially sphere-shaped NCs are observed (Fig. 3a) and a crystalline lattice is noticeable (insert in Fig. 3). The size distribution of $CeAlO_3$ NCs deduced from the analysis of the TEM images is well fitted to a log-normal distribution with an average size of 5.427 ± 1.261 nm. The observed particle size distributions correspond to a log-normal distribution, which is typical for different methods of formation NCs.

For the XRD measurements, the $CeAlO_3$ NCs obtained from the dried colloidal solution, which contained NCs with a size of up to 131 nm, were used. XRD measurements show a main $CeAlO_3$ phase and confirm that PLA-generated $CeAlO_3$ NCs retain their elemental composition and crystalline structure similar to the $CeAlO_3$ single crystal (Fig. 4). No evidence of other phases has been obtained.

For FTIR spectra measurements a single crystal and dried supernatant of $CeAlO_3$ NCs colloidal solutions were used. The FTIR spectrum of $CeAlO_3$ NCs shows the presence of cerium and aluminum oxide peaks in a similar arrangement compared to the bulk material. For $CeAlO_3$ single crystal, FTIR spectrum indicates a 2349 cm^{-1} peak that is related to the presence of carbon–oxygen bonds [19, 20]. The presence of carbon can be related to the Ar + CO atmosphere that was used for crystal growth [9, 10]. It should be noted that after PLA, the peak which corresponded to carbon–oxygen bonds is not observed in the FTIR spectrum of $CeAlO_3$ NCs (Fig. 5). The mechanisms of carbon disappearance in PLA-synthesized NCs will be the subject of further research.

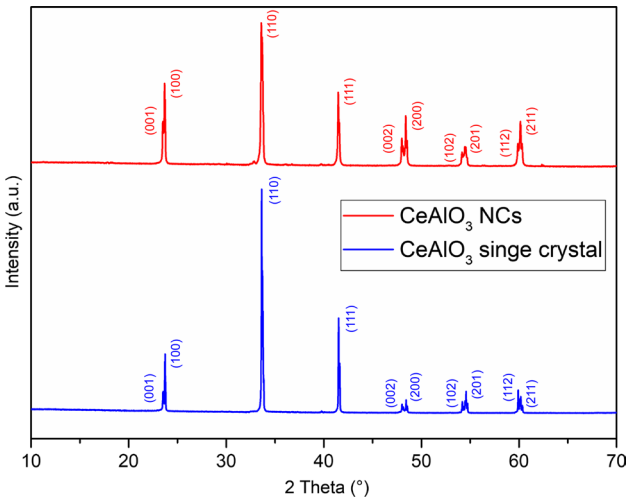

Fig. 4 XRD analysis of $CeAlO_3$ NCs (red) and $CeAlO_3$ single crystal (blue)

3.2 Optical properties

The absorption spectrum (Fig. 6a) and luminescent spectra (Fig. 6b) ($\lambda_{ex} = 260$ nm, 350 nm) of $CeAlO_3$ NCs colloidal solution in chloroform were measured. $CeAlO_3$ NCs demonstrate absorption in the short wavelength range up to 400 nm with weak maximums at 250, 293,350 nm which is very close to the absorption of $CeAlO_3$ bulk crystal in [9]. The absorption spectrum shows that peaks of $CeAlO_3$ NCs colloidal solution coincide with absorption spectrum peaks of the $CeAlO_3$ single crystal which are described in [9, 10]. The luminescence spectra of $CeAlO_3$ NCs colloidal solution show a band with

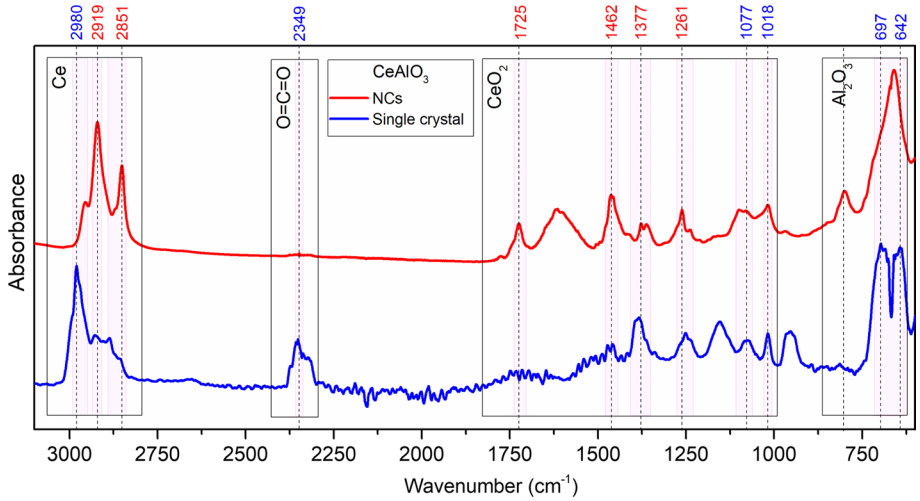

Fig. 5 FTIR spectra of $CeAlO_3$ NCs (red) and $CeAlO_3$ single crystal (blue)

the main peaks at 427 and 437 nm depending on the excitation wavelength. The position of the luminescence maximum of NCs is consistent with the position of the luminescence maximum for the $CeAlO_3$ single crystal [9]. However, such long-wavelength luminescence is attributed to the luminescence of an uncontrolled impurity, which is the phase $CeAl_{11}O_{18}$ [9, 10], that can form in the system Ce_2O_3-Al_2O_3 [21] and it is difficult to determine by XRD due to, probably, low concentration. A similar long-wavelength luminescence was observed in cerium-activated lanthanum-aluminum perovskite crystals, and it was also attributed to the emission of impurity centers $LaAl_{11}O_{18}$ [22].

The luminescence decay curve of $CeAlO_3$ NCs was measured at the excitation wavelength of 270 nm and is shown in Fig. 6c. The decay curve is not mono-exponential with the best approximation by two exponents and reveals the following decay times and fractional amplitudes components: $\tau_1 \sim 1.5$ ns (71%), $\tau_2 \sim 10$ ns (29%) with $\tau_{av} \sim 4$ ns (amplitude weighted), which is typical for the Ce^{3+} decay time in perovskite hosts [9, 11]. However, the value of the average luminescence decay time of $CeAlO_3$ single crystal is equal to $\tau_{av} \sim 16$ ns [9], which is an order of magnitude greater than the observed value $\tau_1 \sim 1.5$ ns of the short luminescence decay time of $CeAlO_3$ NCs. The very fast luminescence process of $CeAlO_3$ NCs is most likely due to the presence of defects, such as traps, which is typical for a highly defective NC structure [23]. Considering the $\tau_2 \sim 10$ ns component, these values are not very far from those observed for the Ce^{3+} 5d–4f emission in the perovskite lattice [9, 22, 24].

4 Conclusions

For the first time, colloidal solutions of pure $CeAlO_3$ NCs have successfully been generated by PLA technique. The usage of chloroform as the most suitable liquid medium for PLA synthesis has been demonstrated. Characterization of the obtained nanoparticles has shown that $CeAlO_3$ NCs did not lose their optical properties compared to the initial $CeAlO_3$ single crystal. In $CeAlO_3$ NCs, shortening of the luminescence decay times compared to the bulk material has been observed, which is important for the development of fast scintillation detectors.

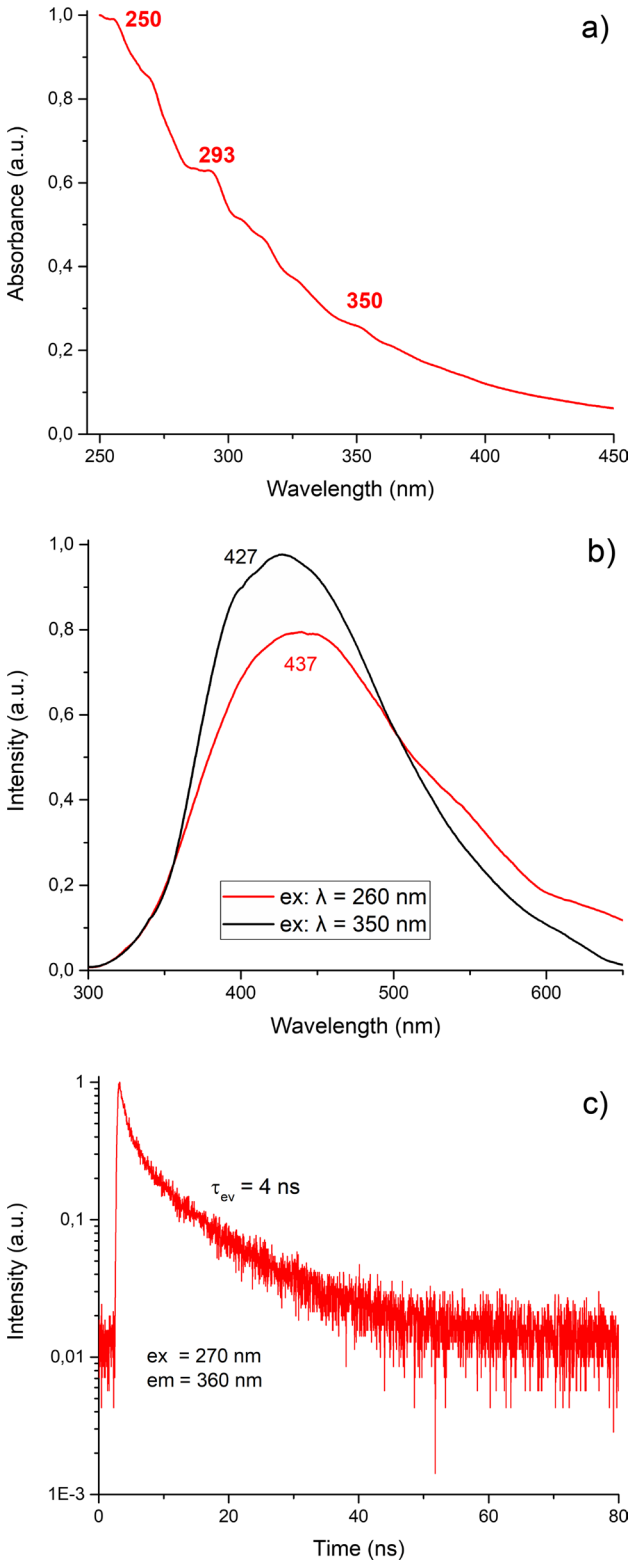

Fig. 6 **a** Absorption spectrum of $CeAlO_3$ NCs colloidal solution in chloroform (red); **b** Luminescence spectra of $CeAlO_3$ NCs colloidal solution in chloroform; **c** Luminescent decay times of $CeAlO_3$ colloidal solution in chloroform

Acknowledgements This work was supported by the Federal Ministry of Education and Research of Germany in the framework of the project "German-Ukrainian Cores of Excellence" – «NanoScint» (01DK21007), and German Academic Exchange Service – "Research Grants—Short-Term Grants" (57552337). Thanks go to the Laboratory of Nano and Quantum Engineering (LNQE) of Leibniz University Hannover for the possibility of conducting TEM measurements. The authors also acknowledge the group of Prof. Dr. Alexander Heisterkamp at the Lower Saxony Center for Biomedical Engineering, Implant Research and Development for assistance with FTIR measurements.

Author contributions VV: conceptualization, investigation, writing—original draft, visualization, writing—review and editing; IB: conceptualization, investigation, and writing—original draft; OG: investigation, writing—review and editing; MS: investigation and supervision; ST: crystal growth; PA: investigation and crystal growth; IG: investigation, crystal growth, writing—review and editing; YZ: investigation; ZZ: XRD measurements and data analysis; AF: conceptualization of XRD measurements and Funding acquisition; AS: luminescence decay times measurements; OS: investigation and funding acquisition; BG: investigation and supervision; BC: supervision, writing—review and editing, funding acquisition.

Funding Open Access funding enabled and organized by Projekt DEAL.

Data availability The data obtained and/or analyzed during the study are not publicly available but are available from the corresponding author upon reasonable request.

Declarations

Conflict of interest The authors declare that they have no conflict of interest.

References

1. C.-Y. Shih, M.V. Shugaev, C. Wu, L.V. Zhigilei, The effect of pulse duration on nanoparticle generation in pulsed laser ablation in liquids: insights from large-scale atomistic simulations. Phys. Chem. Chem. Phys. **22**(13), 7077–7099 (2020). https://doi.org/10.1039/d0cp00608d
2. D. Zhang, B. Gökce, S. Barcikowski, Laser synthesis and processing of colloids: fundamentals and applications. Chem. Rev. **117**(5), 3990–4103 (2017). https://doi.org/10.1021/acs.chemrev.6b00468
3. A.H. Attallah, F.S. Abdulwahid, Y.A. Ali, A.J. Haider, Effect of liquid and laser parameters on fabrication of nanoparticles via pulsed laser ablation in liquid with their applications:

a review. Plasmonics (2023). https://doi.org/10.1007/s11468-023-01852-7
4. V. Amendola, M. Meneghetti, What controls the composition and the structure of nanomaterials generated by laser ablation in liquid solution? Phys. Chem. Chem. Phys. **15**(9), 3027–3046 (2013). https://doi.org/10.1039/c2cp42895d
5. V. Vasylkovskyi et al., Laser synthesis of cerium-doped garnet nanoparticles. Nanomaterials **13**(15), 2161 (2023). https://doi.org/10.3390/nano13152161
6. C.L. Sajti, R. Sattari, B.N. Chichkov, S. Barcikowski, Gram scale synthesis of pure ceramic nanoparticles by laser ablation in liquid. The Journal of Physical Chemistry C **114**(6), 2421–2427 (2010). https://doi.org/10.1021/jp906960g
7. D. Amans et al., Synthesis of oxide nanoparticles by pulsed laser ablation in liquids containing a complexing molecule: impact on size distributions and prepared phases. The Journal of Physical Chemistry C **115**(12), 5131–5139 (2011). https://doi.org/10.1021/jp109387e
8. G. Ledoux, D. Amans, C. Dujardin, and K. Masenelli-Varlot, "Facile and rapid synthesis of highly luminescent nanoparticles via pulsed laser ablation in liquid," Nanotechnology, vol. 20, no. 44, p. 445605, Oct. 2009, doi: https://doi.org/10.1088/0957-4484/20/44/445605
9. O. Sidletskiy et al., Luminescent and scintillation properties of $CeAlO_3$ crystals and phase-separated $CeAlO_3$/$CeAl_{11}O_{18}$ metamaterials. Crystals **9**(6), 296 (2019). https://doi.org/10.3390/cryst9060296
10. P. Arhipov et al., Growth and characterization of large $CeAlO_3$ perovskite crystals. J. Cryst. Growth **430**, 116–121 (2015). https://doi.org/10.1016/j.jcrysgro.2015.08.025
11. Y. Zorenko et al., Growth and luminescent properties of single crystalline films of Ce^{3+} doped Pr1−xLuxAlO$_3$ and Gd1−xLuxAlO$_3$ perovskites. J. Cryst. Growth **457**, 220–226 (2017). https://doi.org/10.1016/j.jcrysgro.2016.02.020
12. R. A. Rajan, H. Tao, W. Yu, and J. Yang, "Space-resolved light emitting and lasing behaviors of crystalline perovskites upon femtosecond laser ablation," Materials Today Physics, vol. 31, p. 101000, 2023, doi: https://doi.org/10.1016/j.mtphys.2023.101000
13. S.T. Aruna, N.S. Kini, S. Shetty, K.S. Rajam, Synthesis of nanocrystalline CeAlO3 by solution-combustion route. Mater. Chem. Phys. **119**(3), 485–489 (2010). https://doi.org/10.1016/j.matchemphys.2009.10.001
14. K. Kamonsuangkasem, S. Therdthianwong, A. Therdthianwong, N. Thammajak, Remarkable activity and stability of Ni catalyst supported on CeO_2-Al_2O_3 via $CeAlO_3$ perovskite towards glycerol steam reforming for hydrogen production. Appl. Catal. B **218**, 650–663 (2017). https://doi.org/10.1016/j.apcatb.2017.06.073
15. I. Luisetto, S. Tuti, C. Battocchio, S. Lo Mastro, and A. Sodo, "Ni/CeO2–Al2O3 catalysts for the dry reforming of methane: The effect of $CeAlO_3$ content and nickel crystallite size on catalytic activity and coke resistance," Applied Catalysis A: General, vol. 500, pp. 12–22, 2015, doi: https://doi.org/10.1016/j.apcata.2015.05.004
16. Z. Zhang, G. Zhao, W. Li, J. Zhong, and J. Xie, "Key properties of Ni/CeAlO3-Al2O3/SiC-foam catalysts for biogas reforming: Enhanced stability and CO_2 activation," Fuel, vol. 307, p. 121799, 2022, doi: https://doi.org/10.1016/j.fuel.2021.121799
17. F. Shahverdi, A. Barati, E. Salehi, M. Arjomandzadegan, Biaxial electrospun nanofibers based on chitosan-poly (vinyl alcohol) and poly (Ɛ-caprolactone) modified with $CeAlO_3$ nanoparticles as potential wound dressing materials. Int. J. Biol. Macromol. **221**, 736–750 (2022). https://doi.org/10.1016/j.ijbiomac.2022.09.061
18. Yu. T. Zholudov, C. L. Sajti, N. N. Slipchenko, and B. N. Chichkov, "Generation of fluorescent CdSe nanocrystals by short-pulse laser fragmentation," Journal of Nanoparticle Research, vol. 17, no. 12, 2015, doi: https://doi.org/10.1007/s11051-015-3303-z
19. John Wiley & Sons, Inc. "SpectraBase", https://spectrabase.com/
20. Merck "IR Spectrum Table", https://www.sigmaaldrich.com/DE/en/technical-documents/technical-article/analytical-chemistry/photometry-and-reflectometry/ir-spectrum-table
21. T. Zhang, Y. Li, H. Mu, C. Liu, M. Jiang, Influence of Mg/Ti complex addition on evolution and thermodynamics of the inclusion in Al-killed steel. Metallurgical Research & Technology **114**(3), 306 (2017). https://doi.org/10.1051/metal/2017021
22. J. Pejchal et al., Untangling the controversy on Ce3+ luminescence in LaAlO3 crystals. Materials Advances **3**(8), 3500–3512 (2022). https://doi.org/10.1039/d1ma01083b
23. M.I. Bodnarchuk, E.V. Shevchenko, D.V. Talapin, Structural defects in periodic and quasicrystalline binary nanocrystal superlattices. J. Am. Chem. Soc. **133**(51), 20837–20849 (2011). https://doi.org/10.1021/ja207154v
24. A.A. Setlur, U. Happek, Cerium luminescence in nd0 perovskites. J. Solid State Chem. **183**(5), 1127–1132 (2010). https://doi.org/10.1016/j.jssc.2010.03.025